

Обзор ArXiv/astro-ph, 6-10 апреля 2020

От Сильченко О.К.

ArXiv: 2004.04363

Volumetric Star Formation Prescriptions in Vertically Resolved Edge-on Galaxies

Kijeong Yim,^{1*} Tony Wong,² Richard J. Rand,³ Eva Schinnerer⁴

¹*Korea Astronomy and Space Science Institute, 776 Daedeok-daero, Yuseong-gu, Daejeon 34055, Korea*

²*Department of Astronomy, University of Illinois, 1002 West Green Street, Urbana, IL 61801, USA*

³*Department of Physics and Astronomy, University of New Mexico, 1919 Lomas Blvd NE, Albuquerque, NM 87131-1156, USA*

⁴*Max Planck Institute für Astronomie, Königstuhl 17, D-69117, Heidelberg, Germany*

Accepted 2020 April 03. Received 2020 April 02; in original form 2019 January 22

ABSTRACT

We measure the gas disc thicknesses of the edge-on galaxy NGC 4013 and the less edge-on galaxies (NGC 4157 and 5907) using CO (CARMA/OVRO) and/or HI (EVLA) observations. We also estimate the scale heights of stars and/or the star formation rate (SFR) for our sample of five galaxies using *Spitzer* IR data (3.6 μm and 24 μm). We derive the average volume densities of the gas and the SFR using the measured scale heights along with radial surface density profiles. Using the volume density that is more physically relevant to the SFR than the surface density, we investigate the existence of a volumetric star formation law (SFL), how the volumetric SFL is different from the surface-density SFL, and how the gas pressure regulates the SFR based on our galaxy

Галактики выборки

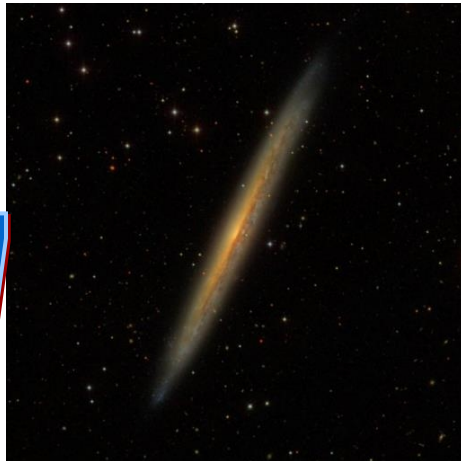
NGC 4013



NGC 4565



NGC 5907



NGC 4157



и еще NGC 891...

NGC 4013

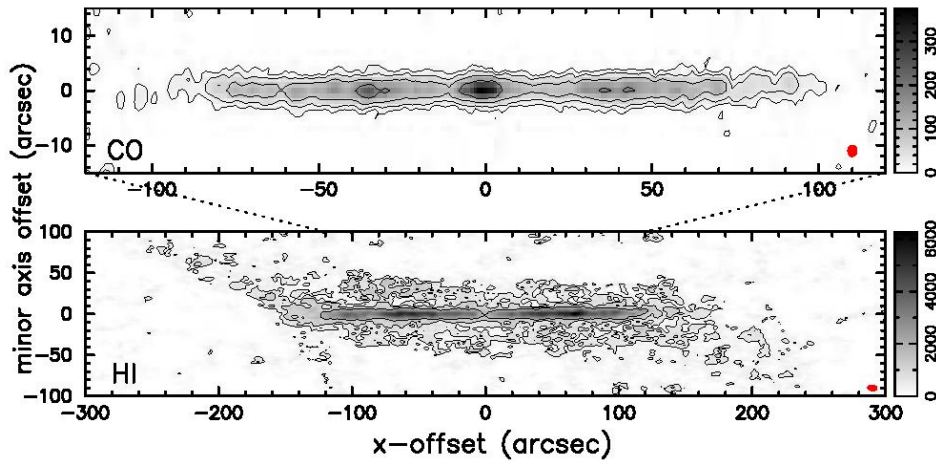


Figure 1. CO (top) and HI (bottom) integrated intensity maps of NGC 4013. Contour levels are $15.0 \times 2.2''$ K km s⁻¹, with n=0, 1, 2, 3 for CO and $450.0 \times 2.0''$ K km s⁻¹, with n=0, 1, 2 for HI. The lowest contour level is $\sim 3\sigma$. The synthesized beam is shown in the lower right corner of each panel.

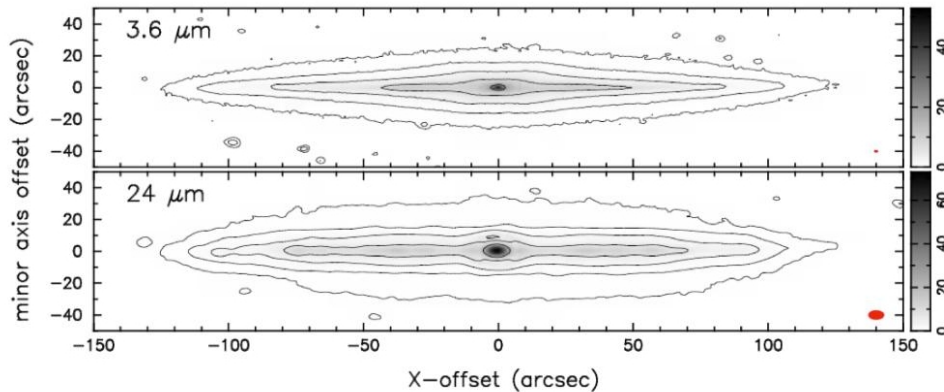


Figure 2. The *Spitzer* 3.6 μ m (top) and 24 μ m (bottom) images of NGC 4013. Contour levels are $0.2 \times 3.25''$ MJy sr⁻¹, with n=0, 1, 2, 3, 4. The point-spread function of the images is shown in the lower right corner of each panel: $1.66'' \times 1.66''$ for 3.6 μ m and $5.90'' \times 5.90''$ for 24 μ m.

- Газ
- Молекулярный
- И нейтральный водород

- Звезды
- Горячая пыль (SFR)

A NGC 4157 и NGC 5907 перенаблюдали на EVLA с разрешением 5''

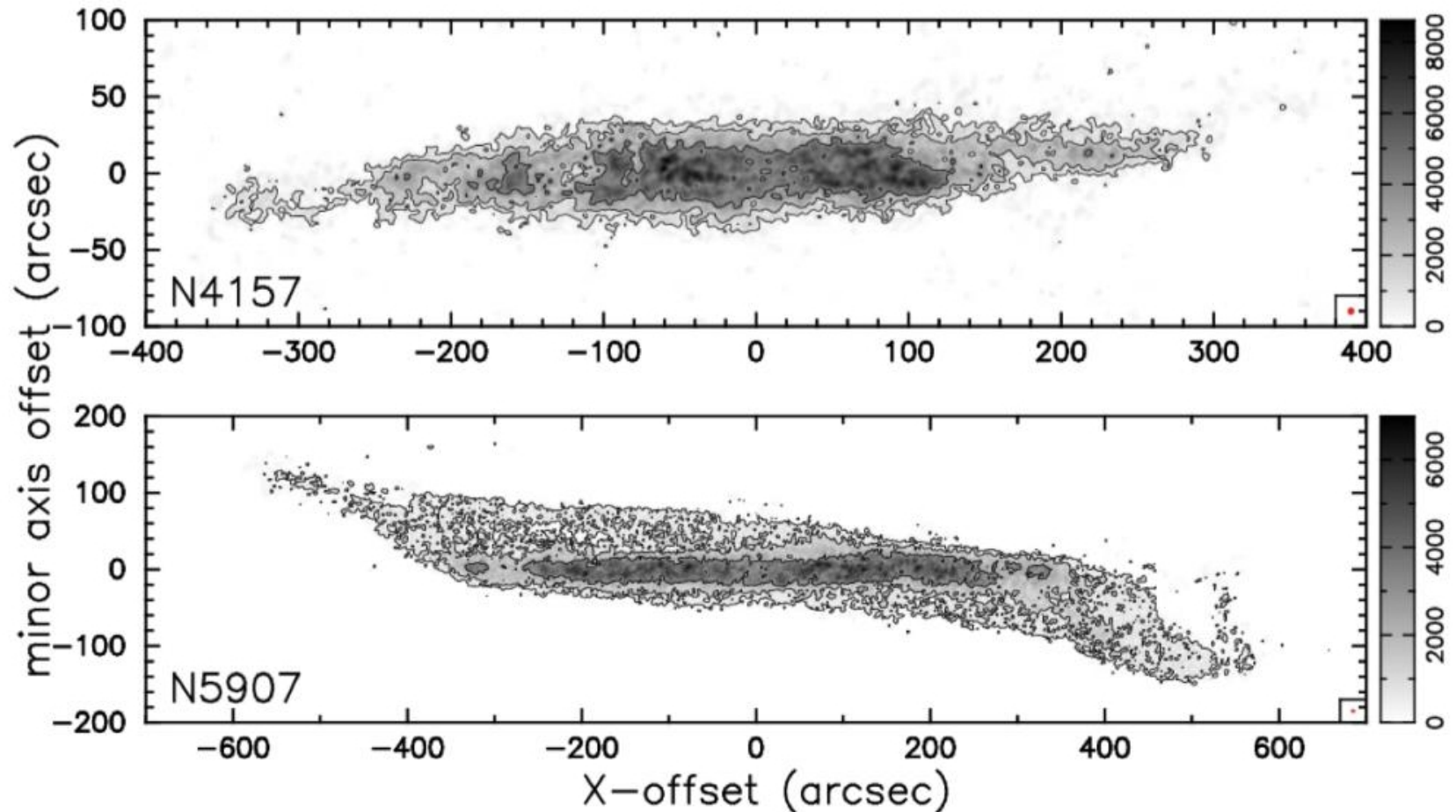


Figure 3. HI integrated intensity maps of NGC 4157 (top) and NGC 5907 (bottom). Contour levels are $750 \times 2.3''$ K km s^{-1} , with $n=0, 1, 2$ for NGC 4157 and $360 \times 2.7''$ K km s^{-1} , with $n=0, 1, 2$ for NGC 5907. The lowest contour level is 3σ . The synthesized beam is shown in the lower right corner of each panel.

Кривая вращения NGC 4013

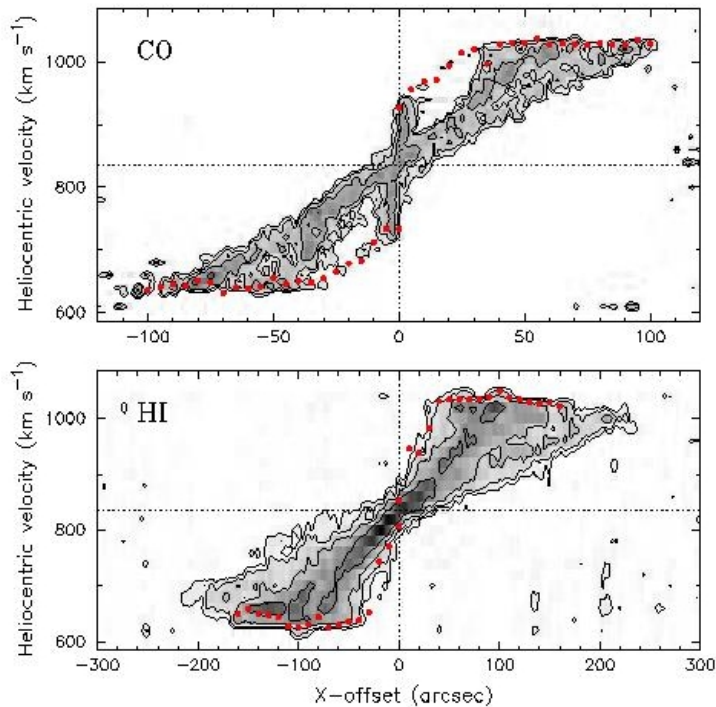


Figure 4. Vertically integrated position-velocity diagrams of NGC 4013 CO (top) and HI (bottom) line emission. CO contours are $2.4 \times 1.8''$ K arcsec, with $n=0, 1, 2, 3$. HI contour levels are $90.0 \times 2.1''$ K arcsec, with $n=0, 1, 2, 3$. The lowest contour level is 3σ . The horizontal dotted lines indicate the heliocentric systemic velocity of 835 km s^{-1} . The red circles represent the obtained rotation velocities.

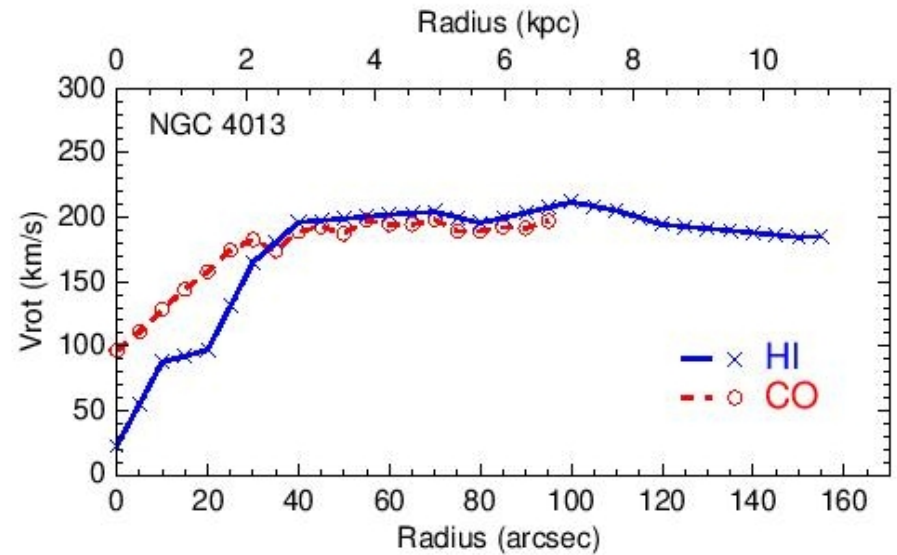


Figure 5. Rotation curves of CO (red circle) and HI (blue cross) for NGC 4013.

Профили пов. Плотности с программой RADPROF

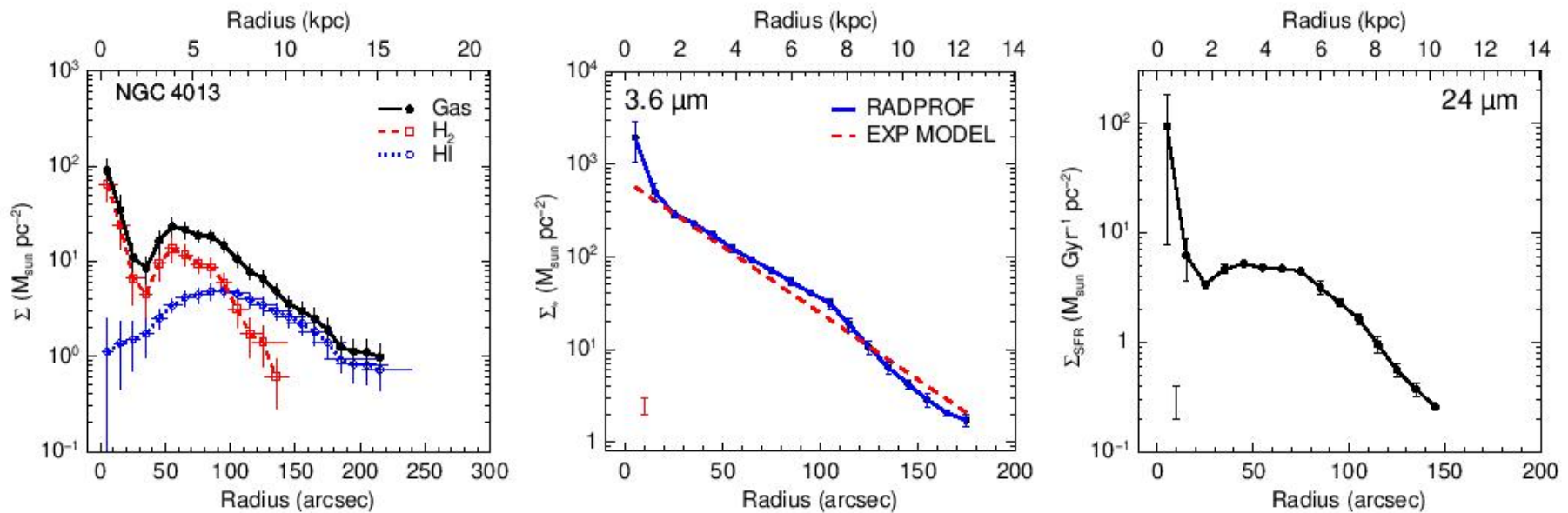


Figure 6. Left: Radial distributions of Σ_{H_2} (red open squares), Σ_{HI} (blue open circles), and Σ_{gas} (solid circles). The vertical error bars are the standard deviation of data points in the radial bins. Middle: stellar surface density profiles obtained from the GIPSY task RADPROF (blue solid line) and the exponential disc model (red dashed line). The error bar on the lower left corner represents the largest difference between the RADPROF and the model profiles except the central regions. Right: SFR surface density as a function of radius obtained from *Spitzer* $24 \mu\text{m}$ imaging using RADPROF. The vertical error bars on the RADPROF profile show the standard deviation of each point. The vertical error bar on the lower left corner shows a factor of 2 uncertainty obtained by comparing two different radial profiles from the RADPROF and ELLINT tasks.

Толщины газовых и звездного ДИСКОВ для NGC 4013

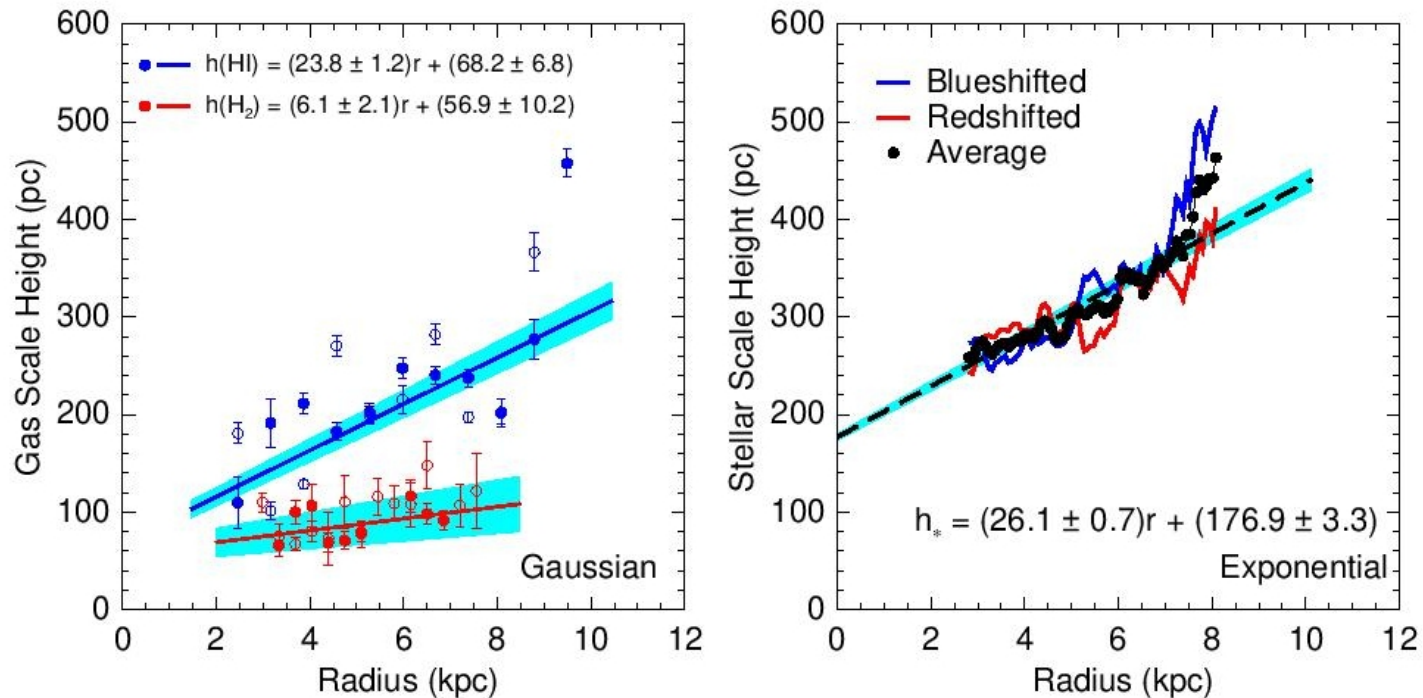


Figure 8. Left: Molecular (red) and atomic (blue) gas scale heights in NGC 4013 as a function of radius measured by fitting a Gaussian function to the vertical profiles of CO and H I. The open and filled circles show the blue-shifted and redshifted sides, respectively. The vertical error bars show uncertainties of the nonlinear least-squares fit to the Gaussian function for the scale heights. The lines are linear least-squares fits to all the data points and the fitting functions are shown on the top. The shaded regions around the lines represent uncertainties of the best-fits. Right: Stellar scale height in NGC 4013 as a function of radius obtained by fitting an exponential function to the vertical profiles of $3.6 \mu\text{m}$. The red and blue lines show the blue-shifted and redshifted sides, respectively. The filled circles are average values of both sides. The dashed line is the best fit (shown on the bottom) to the average values and the shaded region shows the uncertainty of the fit.

Отступление для Насти Каспаровой: косеканс или экспонента?

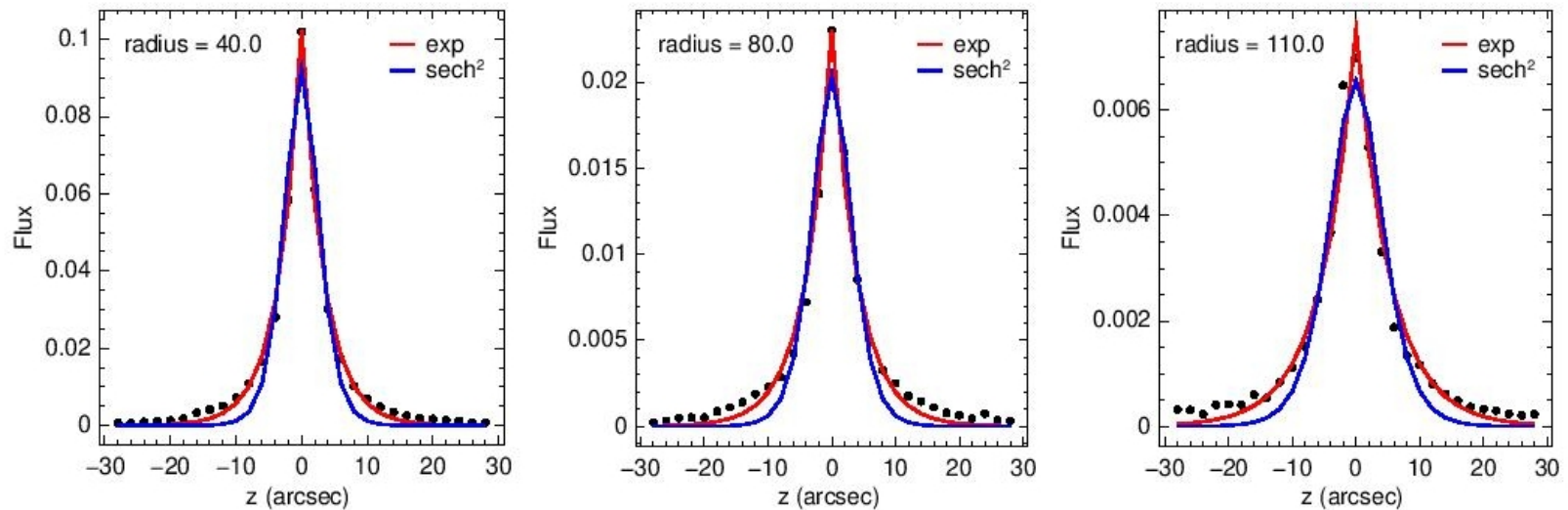
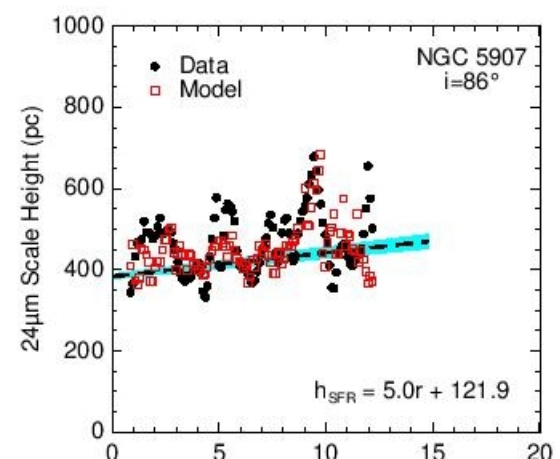
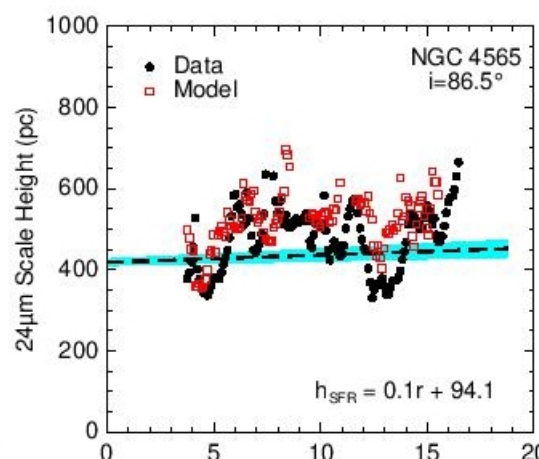
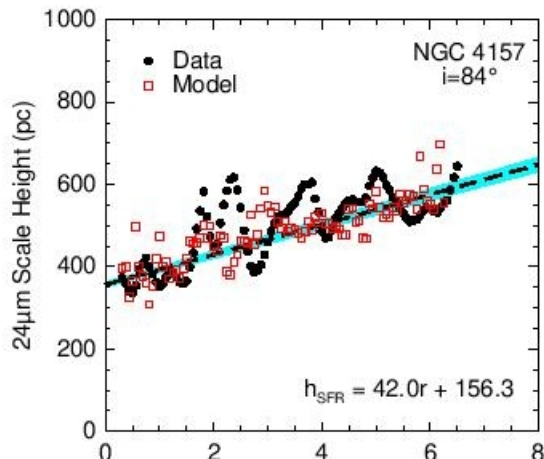
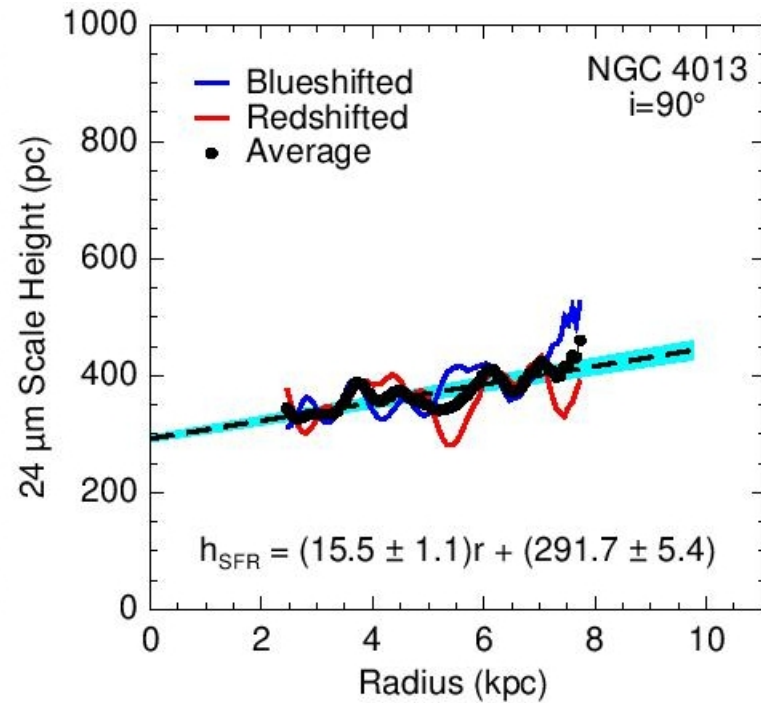
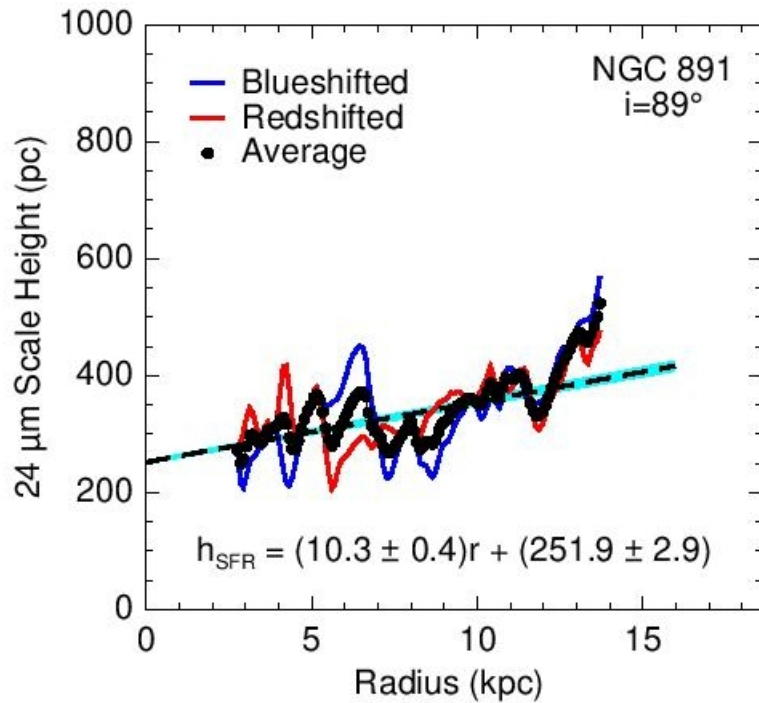


Figure 9. Exponential (red line) and sech^2 (blue line) fitting in NGC 4013 to the vertical profiles (filled circles) of $3.6 \mu\text{m}$ at radius $40''$ (left), $80''$ (middle), and $110''$ (right).

И статистика толщин SFR



Закон К-S для NGC 4013...

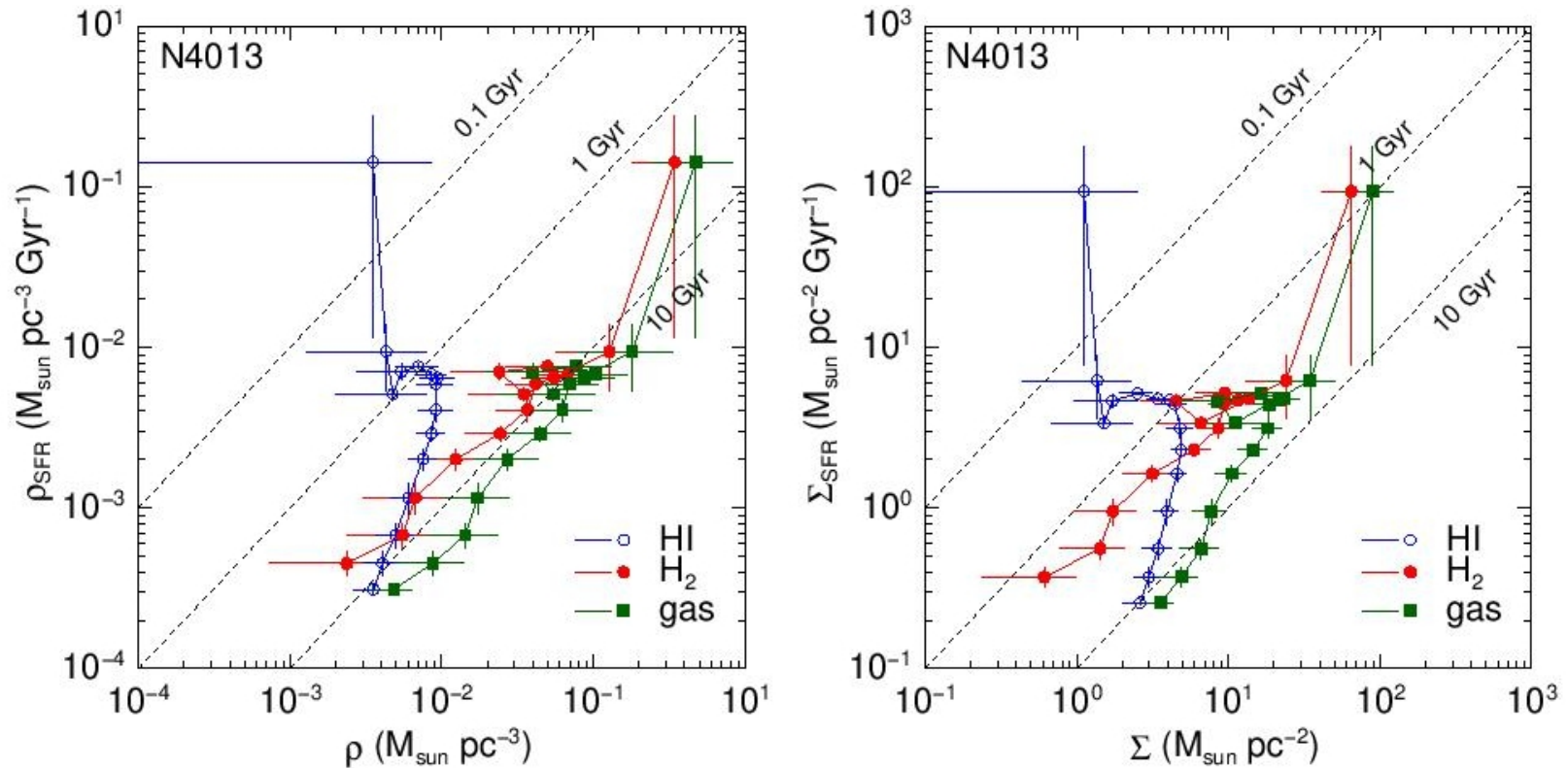


Figure 14. Left: SFR volume density against H₂ (red filled circle), H I (blue open circle), and total gas (green filled square) volume densities of NGC 4013. The vertical and horizontal error bars represent the uncertainties of the volume densities. Right: Σ_{SFR} as a function of Σ_{H_2} , Σ_{HI} , and Σ_{gas} for NGC 4013. The dashed lines show constant SFE and the gas depletion time (SFE^{-1}) is labelled for the lines. The vertical and horizontal error bars represent the uncertainties of the surface densities.

... И ДЛЯ ВСЕХ ОСТАЛЬНЫХ

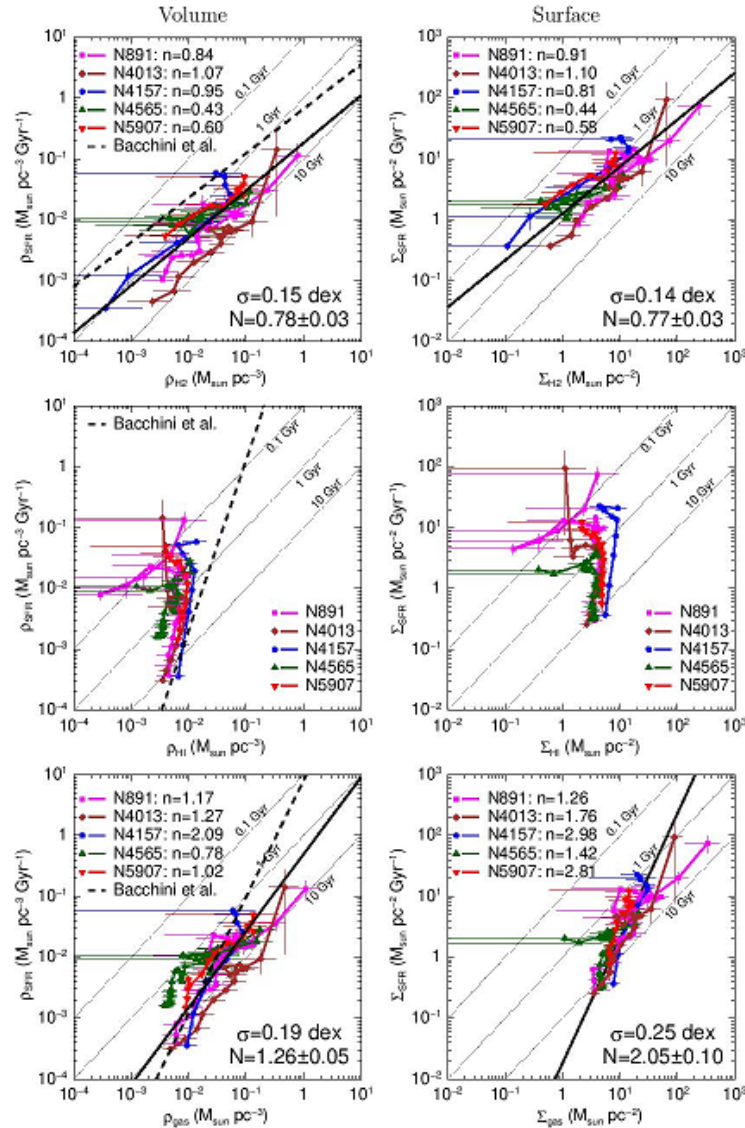


Figure 15. Relationship between SFR and H_2 (top), $H\text{I}$ (middle), and total gas (bottom) based on volume (left-hand panels) and surface (right-hand panels) densities for our galaxy sample. Each power-law index is indicated in the upper-left corner and an average index (black solid line) and rms scatter are presented in the lower-right corner (except for $H\text{I}$). The dashed lines in the volumetric relations are

Размер диска с доминированием молекул на самом деле БОЛЬШЕ!

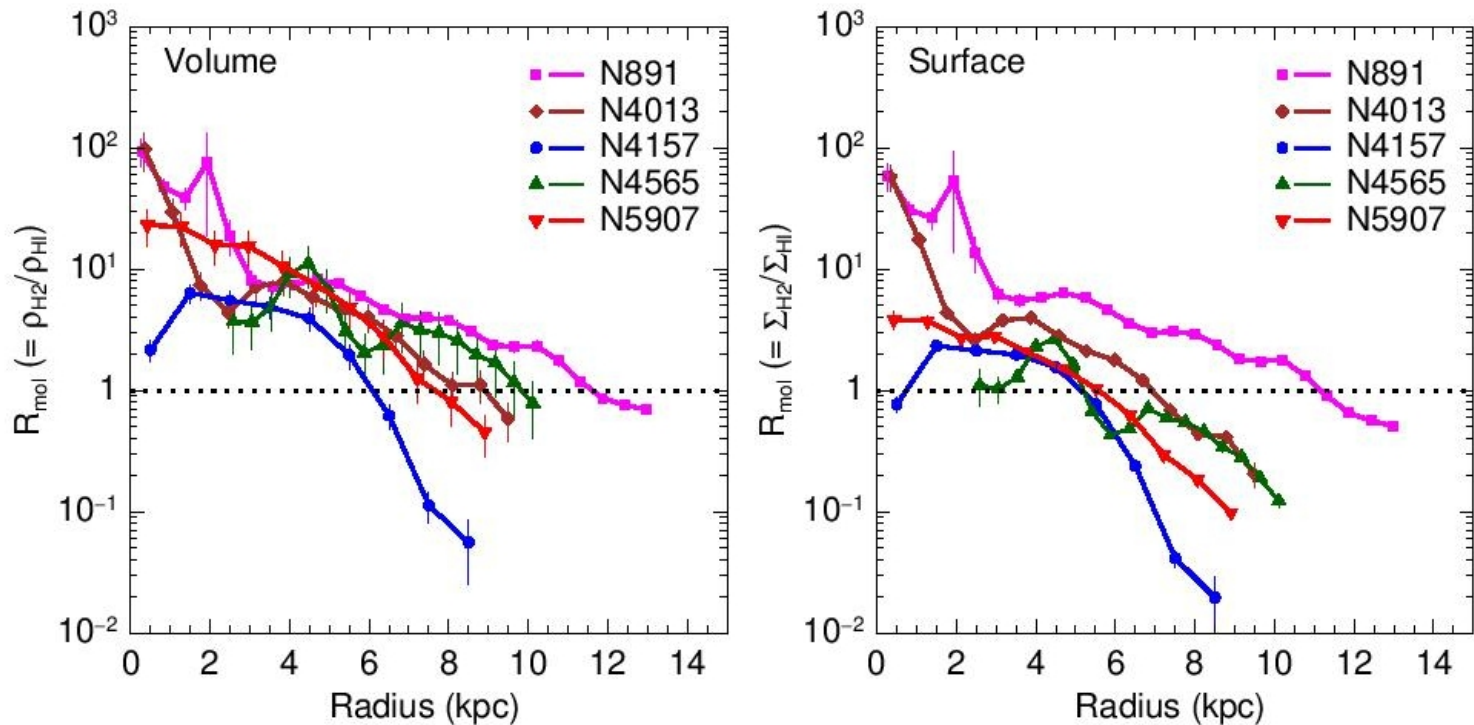


Figure 16. The ratio of molecular to atomic gas as a function of radius for volume (left) and surface (right) densities. The horizontal dotted line indicates $R_{\text{mol}} = 1$. The vertical error bars on the data points represent the standard error of the mean.

Вычисление вертикальной дисперсии скоростей...

The direct measurement of the vertical velocity dispersion is not possible for an edge-on galaxy, since the velocity direction is perpendicular to the line of sight. Instead, we inferred the dispersion by solving the Poisson equation assuming hydrostatic equilibrium given by [Narayan & Jog \(2002\)](#):

$$\sigma_i^2 = \frac{4\pi G \rho_{0,\text{tot}} \rho_{0i}}{-(d^2 \rho_i / dz^2)_{z=0}}, \quad (10)$$

where $\rho_i = \rho_{0i}$ and $d\rho_i/dz = 0$ at $z = 0$ (midplane). The subscript i is for the gas (H_2 and H I) or stars (*). The total midplane volume density ($\rho_{0,\text{tot}}$) is a summation of the

the dark matter would not be important in this study. We obtained the volume densities by integrating a Gaussian distribution for gas and an exponential function for stars along the vertical direction:

$$\rho_{0\text{g}} = \frac{\Sigma_{\text{gas}}}{h_{\text{g}} \sqrt{2\pi}}, \quad \rho_{0*} = \frac{\Sigma_*}{2h_*}. \quad (11)$$

The numerical solutions to equation (10) for gas and stars are:

$$\sigma_{\text{g}} = \sqrt{4\pi G h_{\text{g}}^2 \rho_{0,\text{tot}}}, \quad \sigma_* = \sqrt{2\pi G h_*^2 \rho_{0,\text{tot}}}. \quad (12)$$

... И давления на экваторе

pressure is related to SFR. In Fig. 18 (left), we plot Σ_{SFR} as a function of the hydrostatic midplane pressure calculated from equation (13) given by Yim et al. (2011):

$$P_h = 0.89(G\Sigma_*)^{0.5}\Sigma_{\text{gas}}\frac{\sigma_g}{z_*^{0.5}}, \quad (13)$$

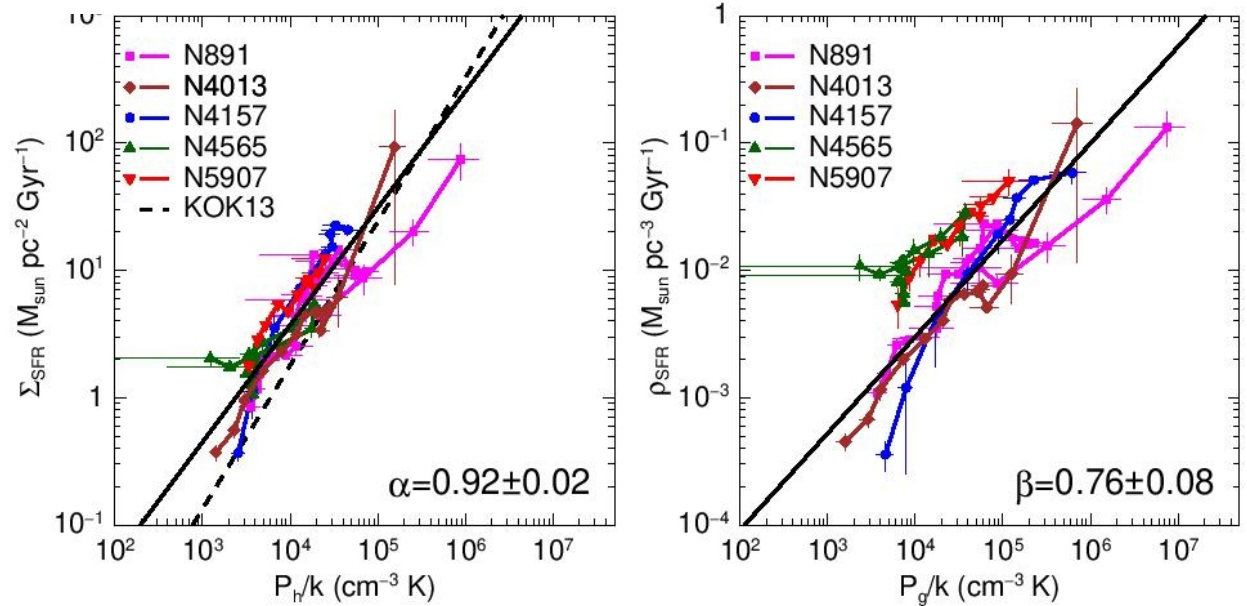


Figure 18. Σ_{SFR} as a function of the hydrostatic midplane pressure (left) and ρ_{SFR} as a function of the interstellar gas pressure (right). The solid line represents an average slope of the five galaxies and the average slope is shown in the lower-right corner. The dashed line in the left panel is the best-fit to simulation data given by Kim et al. (2013) and the power-law slope is 1.13.

R_{mol} and the hydrostatic midplane pressure. The solid line represents the best-fit power law of the galaxy sample and the dashed line shows the best-fit relation from a dynamical equilibrium model provided by Kim et al. (2013) based on three-dimensional numerical hydrodynamic simulations:

$$\frac{\Sigma_{\text{SFR}}}{M_{\odot} \text{ yr}^{-1} \text{ kpc}^{-2}} = 1.8 \times 10^{-3} \left(\frac{P/k_B}{10^4 \text{ cm}^{-3} \text{ K}} \right)^{1.13}. \quad (14)$$